Hindawi Publishing Corporation
Journal of Nanomaterials
Volume 2015, Article ID 463841, 9 pages
http://dx.doi.org/10.1155/2015/463841

Research Article

Interaction between Iron Oxide Nanoparticles and HepaRG Cells: A Preliminary *In Vitro* Evaluation

M. Helvenstein,[1] D. Stanicki,[2] S. Laurent,[2,3] and B. Blankert[1]

[1]*Laboratory of Pharmaceutical Analysis, Faculty of Medicine and Pharmacy, Research Institute for Health Sciences and Technology, University of Mons (UMONS), Place du Parc 20, 7000 Mons, Belgium*
[2]*Department of General, Organic and Biomedical Chemistry, NMR and Molecular Imaging Laboratory, Research Institute for Health Sciences and Technology, University of Mons (UMONS), Place du Parc 20, 7000 Mons, Belgium*
[3]*Center for Microscopy and Molecular Imaging (CMMI), 8 rue Adrienne Bolland, 6041 Gosselies, Belgium*

Correspondence should be addressed to B. Blankert; bertrand.blankert@umons.ac.be

Received 16 January 2015; Revised 4 June 2015; Accepted 2 August 2015

Academic Editor: Ilaria Cacciotti

Nowadays, the use of iron oxide nanoparticles is widespread to label cells for magnetic resonance imaging tracking. More recently, magnetic labeling provides promising new opportunities for tissue engineering by controlling and manipulating cells through the action of an external magnetic field. The present work describes nonspecific labeling of metabolically competent HepaRG hepatocytes with anionic iron oxide nanoparticles. An interaction was observed between nanoparticles and studied cells, which were easily attracted when exposed to a magnet. No cytotoxicity was detected in the hepatocytes after 24 hours of incubation with iron oxide nanoparticles. Impact on HepaRG metabolization activity was assessed. Although a slight decrease in the metabolite generation was observed after exposure to nanoparticles (2 mM in iron), the enzymatic capacity was maintained. These results pave the way for 3D cultures of magnetic labeled HepaRG cells by using a magnetic field.

1. Introduction

The HepaRG cells were isolated from a human hepatocarcinoma and were first described in literature in 2002 [1]. This human hepatic cell line is bipotent and has the ability to differentiate, after treatment during 2 weeks with dimethyl sulfoxide (DMSO), into two different kinds of cells: biliary-like and hepatocyte-like cells [2, 3].

They are principally used to perform drug metabolism and toxicity studies of xenobiotics [4–6]. Indeed, they express and maintain a large panel of phase I enzymes such as CYP 1A2, 2B6, 2C9, 2D6, 2E1, and 3A4 [7, 8]. HepaRG cells also express phase II enzymes (e.g., UGT, GST), transporters, and factors of nuclear transcriptions (e.g., PXR, CAR) [9]. Therefore, the HepaRG cells represent a good alternative to the primary hepatocytes well known for their progressive loss in CYP450 metabolization activity [10]. Among the new innovative strategies developed in predictive drug metabolism profiling in order to reduce this loss of metabolic activity, 3D hepatocyte cultures have been considered. The 3D cell culture approach promotes closer interaction between cells, giving rise to a higher level of cell organization and therefore mimicking in a better way the *in vivo* liver conditions [11]. 3D culture concept in flasks or in bioreactors with the HepaRG cells has also been developed [12–16]. However, 3D and bioreactor cultures still remain challenging and do not yet provide fully competent artificial organs.

Iron oxide nanoparticles (IONPs), coming from the booming nanomaterial area, are nowadays subject to a wide development in biomedical applications such as magnetic drug targeting, gene delivery, therapeutic hyperthermia, or magnetic resonance imaging [17, 18]. During the last decade, an original and promising strategy to build tridimensional culture and tissue engineering has emerged by using magnetic nanoparticles and magnetic force [19–21]. An external magnetic field such as magnets is able to control and drive magnetically labeled cells, resulting in an influence on their organization and their migration [22, 23]. This technology covers a wide range of applications from construction of tubular structures and cardiovascular tissues (localization

of endothelial cells in magnetized stented vessels included) [24–26] to 3D culture of hepatocytes [27]. Some research works described the hepatocytes labeling (mice and Huh7 human hepatoma cell line) by anionic magnetic iron oxide nanoparticles in order to track and to magnetically target them after their transplantation [28, 29].

In this context, we proposed hereafter to study the interaction between HepaRG cell line and anionic iron oxide nanoparticles. Different kinds of experimentations will be performed from magnetic attraction with magnetic field to Prussian blue staining and holographic microscopy. The potential impact on the viability and on the activity of drug metabolization of the studied cell line will also be discussed. To the best of our knowledge, it is the first time that such results are described with the HepaRG cells. Furthermore, IONPs synthesis and characterizations (transmission electron microscopy, hydrodynamic diameter, and zeta potential) will also be briefly presented.

2. Materials and Methods

2.1. Chemicals and Reagents. William's E medium without phenol red, trypsin, potassium ferrocyanide, hydrochloric acid, thiazolyl blue tetrazolium bromide (MTT reagent), dimethyl sulfoxide (DMSO), Dulbecco's Phosphate Buffered Saline (D-PBS), and diclofenac sodium salt were purchased from Sigma-Aldrich (Zwijndrecht, The Netherlands). Sunitinib was supplied from LC Laboratories (Woburn, USA). All cell culture dishes were obtained from Greiner Bio One (Wemmel, Belgium). Acetonitrile and formic acid were purchased from Biosolve BV (Valkenswaard, The Netherlands). Ultrapure water was obtained using a Milli-Q Reference A+ purification system from Merck Milllipore (Overijse, Belgium).

For nanoparticles, ferric chloride solution ($FeCl_3$, 45%), ferrous chloride tetrahydrate ($FeCl_2{\cdot}4H_2O$), and sodium hydroxide were purchased from Fluka (Belgium). Diethylene glycol (DEG), dimethylformamide (DMF), acetone, tetramethylammonium hydroxide pentahydrate (TMAOH), and diethyl ether were purchased from Sigma-Aldrich (Belgium). 3-(triethoxysilyl)propyl succinic anhydride (TEPSA) was purchased from ABCR (Germany). All the materials mentioned above were used without further purification. Membranes (MWCO = 30,000) for ultrafiltration were purchased from Millipore (USA).

2.2. Cell Culture. HepaRG cells were obtained from Biopredic International (Saint-Grégoire, France) and were seeded at low density (2×10^4 cells per cm^2) in 25 cm^2 culture flasks under +37°C and 5% CO_2 atmosphere. As previously described in [30], HepaRG cells present an undifferentiated stage at low density culture. Undifferentiated cells were cultured in growth medium provided from Biopredic International corresponding to William's E medium (WE) supplemented with 10% FBS, 100 units/mL penicillin, 100 μg/mL streptomycin, 5 μg/mL insulin, 2 mM glutamine, and 5×10^{-5} M hydrocortisone hemisuccinate. After 2 weeks, medium was changed to differentiation medium provided by the manufacturer corresponding to enriched William's E medium with 2% DMSO for 2 more weeks. This later medium allows the cell differentiation into biliary-like and hepatocyte-like cells.

2.3. Anionic Iron Oxide Nanoparticles

2.3.1. Synthesis. The synthesis of iron oxide cores and their stabilization with TEPSA have been performed as described previously [31, 32]. Briefly, 8.9 g of ferrous chloride (45 mmol) and 9.1 mL of ferric chloride (37 mmol) in 250 mL of DEG were stirred at 170°C under nitrogen atmosphere. After 15 min, the mixture was stirred in presence of sodium hydroxide (15 g) during 1 h at 170°C. After cooling, and isolation of the magnetic particles from the solution by magnetic decantation, the obtained black precipitate was washed five times with a 1 M aqueous solution of nitric acid (200 mL). In order to eliminate aggregates, magnetite was dispersed in deionized water, sonicated (45 min), and centrifuged (16,500 G; 45 min).

20 mL of the suspension of nanoparticles ([Fe] = 250 mM) was diluted with 50 mL of dimethylformamide and water was eliminated under reduced pressure. 7.1 mL of TEPSA (25 mmol) was slowly added to the dispersion in DMF, followed by 4.3 mL of water and finally by 2.5 mL of an aqueous solution of TMAOH (1 M) at room temperature and under stirring. The solution was heated to 100°C for 24 h. The nanoparticles were collected after pouring the suspension in an acetone/diethyl ether mixture and magnetic decantation. After washing with acetone, the black precipitate was dispersed in water and purified by membrane filtration (membrane cut-off: 30 kDa) and finally centrifuged (16,500 g; 45 minutes).

2.3.2. Physicochemical Characterization Techniques. Transmission electron microscopy (TEM) was carried out on a Fei Tecnai 10 microscope (Oregon, USA) operating at an accelerating voltage of 80 kV. The samples were prepared by placing a drop of diluted IONP suspension on a copper-grid (300 mesh), allowing the liquid evaporation at room temperature. The statistical analysis of the TEM images was performed by iTEM (Germany) on multiple images for each sample. The mean diameter of the core, the standard deviation, and the polydispersity index (PDI) were calculated by measuring the diameter of the IONP. The number of nanoparticles counted ranged from 500 to 700.

The determination of the hydrodynamic diameter and zeta potential of the nanoparticles was performed on a Zetasizer nano zs (Malvern Instruments, United Kingdom) using laser He-Ne (633 nm). The zeta potential was determined directly in aqueous solution containing NaCl (0.01 mM). The aqueous suspension containing the particles was adjusted at different pH values with 0.1–0.001 mM HNO_3 or NaOH solution.

The total iron concentration was determined by measuring the longitudinal relaxation rate R_1 according to the method previously described in [33]. The samples were mineralized by microwave digestion (MLS-1200 Mega, Milestone, Analis, Belgium) and the R_1 value of the resulting

solutions was recorded at 0.47 T and 37°C (Minispec mq 20 spin analyzers, Bruker, Germany), which allowed the determination of iron concentration following the equation

$$[\mathrm{Fe}] = \left(R_{1\,\mathrm{sample}} - R_{1\,\mathrm{diam}}\right) \times 0.0915, \quad (1)$$

where $R_{1\ \mathrm{diam}}$ (s^{-1}) is the diamagnetic relaxation rate of acidified water ($0.36\ \mathrm{s}^{-1}$) and 0.0915 (s·mM) is the slope of the calibration curve.

2.4. Cell Labeling. HepaRG cells were incubated during 17 hours with anionic magnetic nanoparticles at a 2 mM final concentration in iron in serum-free William's E medium without phenol red.

2.4.1. Magnet Attraction. After these 17 hours of incubation, cells were harvested and, once in suspension, a neodymium permanent magnet (Webcraft GmbH, Supermagnete, Germany) was placed near to the culture flask.

2.4.2. Coloration. Prussian blue staining was performed directly into the culture flask. Cells were washed twice with D-PBS and were incubated during 1 minute with a working solution consisting of an equal volume mixing of 10% potassium ferrocyanide in water (m/v) and 7% hydrochloric acid in water (v/v).

Observations were made under inverted microscope surmounted with an Optikam camera (Led Techno, Zolder, Belgium).

2.4.3. Holographic Microscopy. After incubation with IONPs, cells were harvested and replated in order to disperse them. Once cells were adherent into the flask (waiting time of four hours), visualization was realized with a D3HM o-Line microscope (Ovizio, Uccle, Belgium) and analyzed with OsOne 4.3 software (Ovizio, Uccle, Belgium). This technology, in comparison with TEM microscopy, avoids cell pretreatments such as fixation and allows visualization of living cells inside the culture flasks.

2.5. Nanoparticles Toxicity Assessment. HepaRG cells were harvested and seeded at high density (2×10^5 cells per cm^2) in 96-well plates to keep the differentiated stage of the cells and to avoid the dedifferentiation phenomenon.

Cell viability was assessed by MTT cytotoxicity test and realized on two independent experiments in quadruplicate. Cells were incubated with anionic magnetic nanoparticles at different concentrations in iron (from 1 to 5 mM in medium culture) during 24 hours. At this point, they were washed and incubated during 4 hours with MTT solution (thiazolyl blue tetrazolium bromide) at 0.5 mg/mL concentration in D-PBS. Supernatant was replaced by 100 μL DMSO to dissolve the crystals of reduced formazan. Absorbances were measured with a Multiskan Ascent plate reader (Thermo Scientific, Aalst, Belgium) at a selected wavelength of 570 nm versus 690 nm. Statistical analyses (one-way ANOVA followed by Dunnett's posttest) were performed with GraphPad Prism 5 software (GraphPad Software Inc., La Jolla, USA).

2.6. Metabolization Test. After 17 hours of incubation with nanoparticles ($[\mathrm{Fe}]_{\mathrm{medium}} = 2$ mM), HepaRG cells were exposed either to 250 μM diclofenac during 5 hours or to 20 μM sunitinib during 6 hours in serum-free William's E medium without phenol red. Supernatant was removed and mixed with 1/3 volume acetonitrile and centrifuged at 3300 G during 15 minutes at 4°C with a Hettich refrigerated centrifuge (Analis, Suarlee, Belgium).

All metabolization tests results were obtained from four independent cultures and each analysis was performed in triplicate.

Statistical analysis (unpaired t-test) was also realized with GraphPad Prism 5 software (GraphPad Software Inc., La Jolla, USA).

2.6.1. Diclofenac Chromatographic Conditions. Samples were analyzed using a Waters Acquity H-Class UPLC System (Milford, USA) controlled by the Empower software. Metabolites and diclofenac were separated on an Acquity UPLC CSH Phenyl-Hexyl column (1.7 μm; 2.1 × 100 mm) at 40°C. A diode array detector (DAD) was used with the wavelength set at 275 nm. The mobile phase consisted of acetonitrile and water acidified with 0.1% formic acid (v/v). The percentage of acetonitrile was initially set at 43% and constantly increased up to 50% until 4.99 min. Then it was quickly set back to 43% at 5 min and the system was reequilibrated during 1 min before the next injection. The total runtime was 6 min with a flow rate set at 0.5 mL/min.

2.6.2. Sunitinib Chromatographic Conditions. Sunitinib samples were analyzed by the same chromatographic system as diclofenac. A previously developed method by our team was applied [34]. Sunitinib and its metabolite (*N*-desethyl sunitinib) were separated on an Acquity UPLC BEH C18 (1.7 μm; 2.1 × 50 mm) column at 40°C. The mobile phase was made of 4 mM ammonium formate (pH adjusted to 3.2 with formic acid on a Metrohm 827 pH meter (Herisau, Switzerland)) and a combination of 90% acetonitrile/10% 4 mM ammonium formate (pH 3.2). The percentage of this combination was initially set at 5% and immediately increased up to 35% at 0.15 min. Then it was constantly increased up to 37% until 0.8 min and linearly increased up to 90% until 2.9 min. Thereafter it was quickly set back to 5% at 3.02 min until 4 min. Before the next injection, the system was reequilibrated during 1 min. The total run time was 5 min with a flow rate set at 0.4 mL/min. The DAD wavelength was set at 430 nm.

3. Results

3.1. Nanoparticles Preparation and Characterization. As indicated by photocorrelation spectroscopy (PCS; Figure 1), we observed the formation of well-dispersed nanostructures. Furthermore, no aggregation has been noticed after TEPSA treatment. The surface modification could be attested by the observation of shift of the isoelectrical point toward acidic pH (Figure 2). Transmission electron microscopy (TEM; Figure 3) completed the characterization by showing the

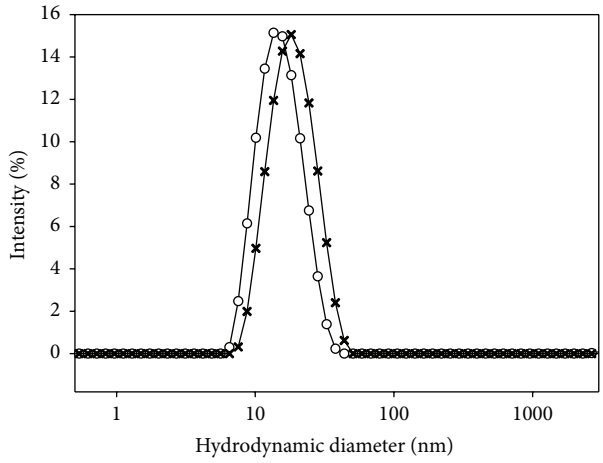

Figure 1: Size distribution in intensity as measured by PCS of uncoated IONPs (o) and TEPSA-coated IONPs (×).

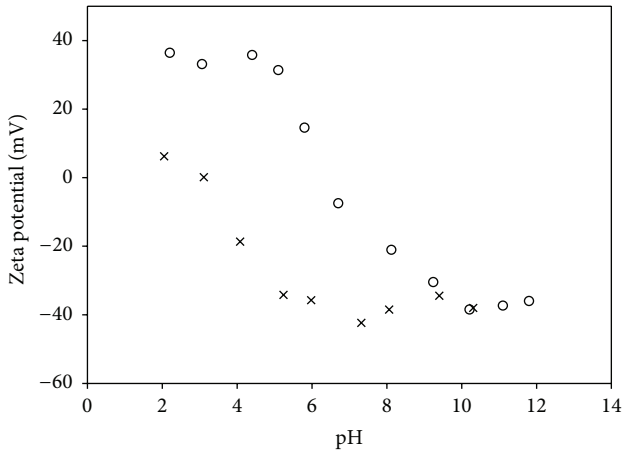

Figure 2: Evolution of the zeta potential with respect to pH for uncoated particles (o) and TEPSA-coated IONPs (×).

formation of quasispherical nanoobjects (d_{mean} = 8.2 nm) characterized by a small polydispersity index (PDI = 1.19).

3.2. Magnetic Attraction. The presence of permanent magnet in the proximity of the culture flask highlighted the interaction between anionic iron oxide nanoparticles and HepaRG cells; labeled cells in suspension exhibited a sensibility to the used magnet. The culture flask was placed on a plastic support (44 × 10 × 4 mm) and on a permanent magnet (40 × 10 × 5 mm). Both were rectangular in shape but the height of the plastic support was inferior (4 mm) to the magnet (5 mm), resulting in an incline of the flask. As shown in Figure 4, the labeled HepaRG cells in suspension were attracted and stayed close to the magnet despite the slope, while unlabeled cells were subject to the slope and moved towards the plastic support. Based on MTT assay results (see Section 3.4) and the lack of medium turbidity (result not shown) before the cell harvest, we assume that the labeled cells were still alive during the magnetic attraction.

These results showed that labeled HepaRG were sensitive to a magnetic field and were consequently trapped in the vicinity of a magnet.

3.3. Prussian Blue Staining. Cells were washed with D-PBS instead of William's E medium without phenol red. Recently, Bridot et al. demonstrated that adsorbed nanoparticles were more effectively washed from the cell surface with phosphate buffer than with the medium itself [32].

As shown in Figure 5, Prussian blue pigmentation clearly revealed a different behavior between magnetically labeled cells and unlabeled cells (Figure 5(a)). Labeled cells (Figure 5(b)) exhibited a dark blue coloration, highlighting the presence of iron oxide nanoparticles (typical reaction between iron and potassium ferrocyanide (Prussian blue precipitate)).

3.4. MTT Assay. Different concentrations in iron (1, 2, 4, and 5 mM) were tested during an incubation time of 24 hours. Viability averages were calculated (see Section 2.5) and showed high percentage values for each tested concentration (Figure 6). Results obtained with one-way ANOVA showed that the variances did not differ significantly ($P > 0.05$). Dunnett's multiple comparison test analyzed each iron concentration versus control. Experimental results for all tested concentrations did not show statistical differences and were nonsignificant (NS, $P > 0.05$). These results indicated that studied anionic magnetic nanoparticles do not seem to present a toxicity effect on HepaRG cells when exposed to a 24-hour incubation time.

3.5. Nanoparticle Internalization. Visualization of nanoparticles inside the HepaRG cells was performed with holographic microscopy technology. Figure 7 shows concentrated nanoparticles (dark points) inside the labeled cells after endocytosis phenomenon. The IONPs are concentrated inside endosomes and allow their observation with this technology.

3.6. Metabolization Test. Diclofenac is a CYP2C9 substrate and its metabolization profile has already been described in HepaRG cells [10].

A typical chromatogram obtained from a sample generated through our metabolization test procedure (see Section 2.6) of 5 hours with a 250 μM diclofenac solution after HepaRG cells interaction in presence or in absence (control) of studied nanoparticles is presented in Figure 8. Metabolites and diclofenac peaks were identified by comparing obtained chromatograms to a blank chromatogram (incubation of 5 hours with William's E serum-free medium without phenol red) and to the typical diclofenac reference compound chromatographic pattern. Metabolite peak areas obtained from sample solutions collected in control situation (no interaction with nanoparticles) were larger than sample solutions collected after exposition and interaction with nanoparticles (Figure 8(a)).

The experimental results were statistically analyzed and diclofenac metabolite peak areas obtained from control experiments were set at 100%. Statistical analysis (unpaired

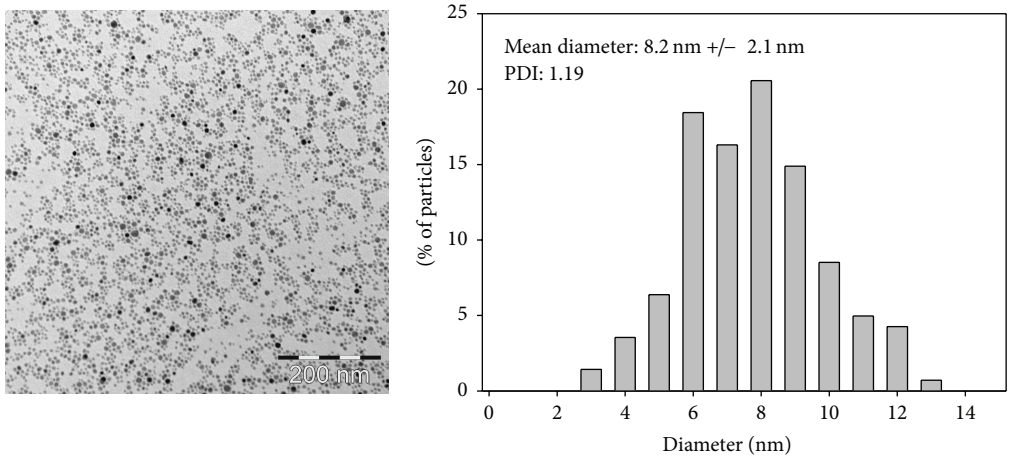

(a) (b)

Figure 3: (a) TEM picture of carboxysilane coated nanoparticles. (b) Statistical analysis revealed the formation of 8.2 nm ± 2.1 nm particle diameter. The size distribution was obtained after a count of more than 500 particles.

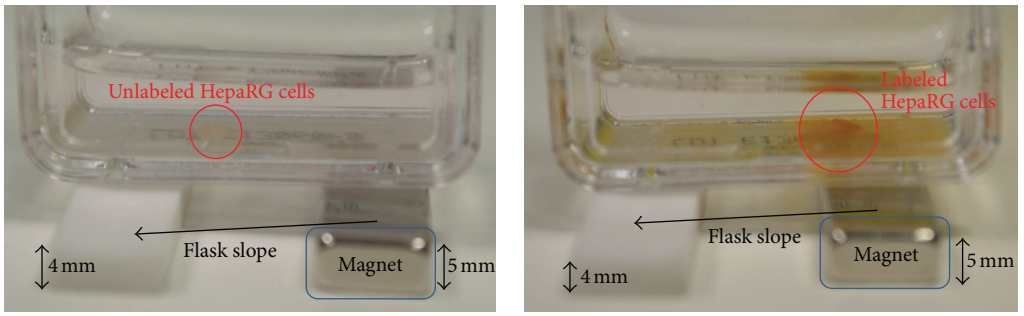

(a) (b)

Figure 4: Cells suspension inside culture flask. (a) Unlabeled cells and (b) magnetically labeled cells after incubation with nanoparticles ([Fe] = 2 mM). Labeled cells in (b) are magnetically held, despite the slope, by the magnet whereas unlabeled cells (a) moved towards the plastic stripe.

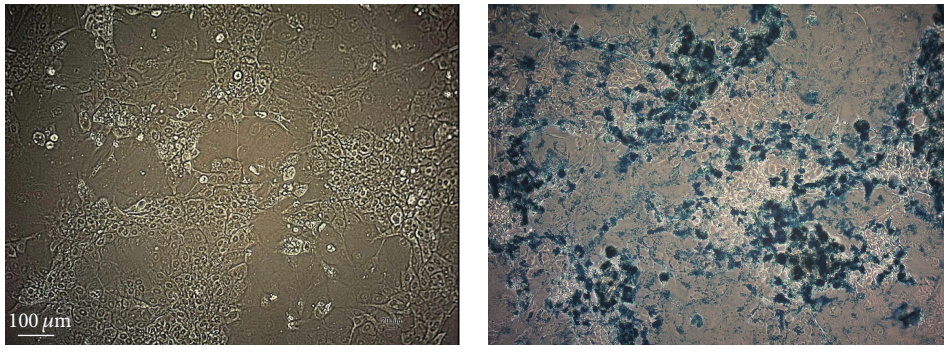

(a) (b)

Figure 5: Prussian blue staining. (a) Control cells: no iron oxide nanoparticle incubation (potassium ferrocyanide solution also present); (b) After 17 hours of incubation with iron oxide nanoparticles ([Fe] = 2 mM), potassium ferrocyanide solution was added. A blue coloring appears in (b) and highlights the presence of iron oxide nanoparticles.

t-test) is shown in Figure 9(a) and expressed a significant difference in cell xenobiotic metabolization level ($^{**}P < 0.01$) between cells incubated either in presence or in absence of iron oxide nanoparticles.

The same methodology was applied to sunitinib metabolization test. This tyrosine kinase inhibitor (TKI) drug is metabolized by the CYP3A4 isoform into a N-desethyl compound [35]. Statistical examination (unpaired t-test) based

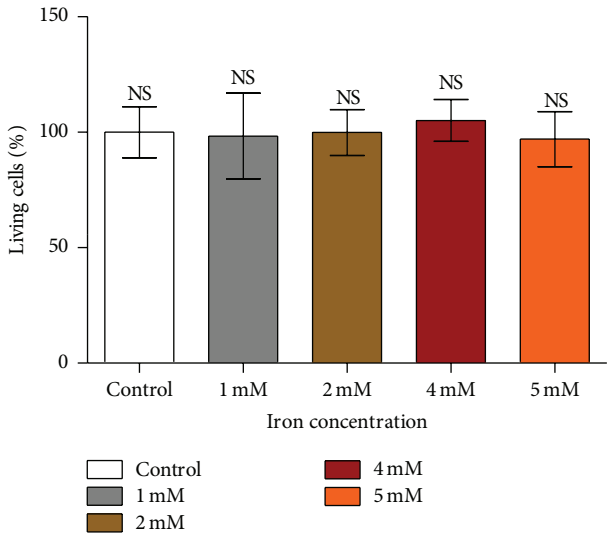

FIGURE 6: Histogram of cell viability percentage for each tested concentration in iron (two independent experiments in quadruplicates). One-way ANOVA test and Dunnett's posttest show no significant difference (NS, $P > 0.05$).

on results extracted from sunitinib analysis (chromatogram at Figure 8(b) (6 hours of metabolization)) expressed a significant difference in cell metabolization activity ($^{***}P < 0.001$) depending on the IONPs exposure (illustrated in Figure 9(b)).

HepaRG cells maintained their metabolization activity after their exposure (17 hours) to iron oxide nanoparticles ([Fe] = 2 mM); however their xenobiotic metabolization activity appears to be slightly decreased.

4. Discussion

In this study, we have evaluated the impact of anionic iron oxide nanoparticles on the viability and the metabolization activity of HepaRG cells. HepaRG cells were selected for their ability to express and to maintain different phase I and phase II enzymes levels during several weeks, making them a useful tool to perform drug metabolism studies [4].

Cell labeling with anionic iron oxide nanoparticles has been described as a phenomenon applicable to all kinds of cells. The interaction of anionic magnetic nanoparticles with cells seems to involve a two-step mechanism. Due to their negative charge, an adsorption phenomenon on the cell surface occurs, described as a Langmuir adsorption in literature. The second step, reported by Wilhelm et al., consists of internalization by the endocytosis pathway [36, 37]. The presence of anionic nanoparticles inside the HepaRG cells was observed via holographic microscopy technology leading us to consider that endocytosis phenomenon was effectively performed by this cell line.

Based on magnetic iron oxide properties, labeled cells can easily be moved when exposed to an external magnetic field such as magnet [38]. As expected, we observed (Figure 4) that the magnetically labeled HepaRG cells in suspension were held by the presence of a permanent magnet at the top of the culture flask despite its slope. These results demonstrated the concrete interaction between anionic iron oxide nanoparticles and the HepaRG cell line. Prussian blue staining confirmed the IONPs/cells interaction unlike the cells not incubated with IONPs (Figure 5).

Evaluation of the potential cytotoxicity resulting from iron oxide nanoparticle exposure represents a key point to assess. It is well established that one of the most important nanotoxicity mechanisms is the production of reactive oxygen species (ROS), by Fenton or Haber-Weiss reactions. The generation of ROS can induce oxidative stress to cells leading to different kinds of nanotoxicity such as cell death, lipid peroxidation, DNA, and mitochondrial damages [39, 40].

Based on usual iron concentrations reported in retrieved publications, different concentrations (1, 2, 4, and 5 mM) were tested to evaluate the HepaRG cell viability using a MTT assay [28, 29]. Furthermore, described incubation times vary from few minutes to several hours for biomedical applications [38]. Therefore, we considered an incubation time of 24 hours to assess the potential toxicity. The obtained data (Figure 6) indicated that studied anionic magnetic nanoparticles did not show any cytotoxicity ($P > 0.05$) against HepaRG cells. By extrapolation, shorter incubation times should not lead to toxic effect on the cells.

As explained in the Introduction, an original way to exploit magnetic IONPs is the control of organization and migration of magnetically labeled cells. Based on magnetic properties of iron oxide, labeled cells are easily driven when submitted to a magnetic field (magnet). This property allows perspectives in tissue engineering and regenerative medicine [22].

The use of magnetically labeled hepatocyte cell lines has been described in literature. Human hepatoblastoma HepG2 cell line was integrated in a magnetic force-based 3D coculture system with mouse fibroblasts [27]. Furthermore, transplantations of magnetically labeled liver cells have been successfully performed in mice with Huh7 human hepatoma cell line and mouse hepatocytes [28, 29].

Although the toxicity aspects are often studied, IONPs impact on cell enzymes is less investigated. In this context, we realized metabolization tests using diclofenac and sunitinib as reference substances. A significant small decrease in metabolization activity has been observed (regarding both studied xenobiotics) between control samples and labeled HepaRG cells (Figure 9). Of course, these preliminary results should be compared and confirmed with metabolization tests involving other drugs. This IONP impact on cytochrome P450 activity should be more investigated and kept in mind for future investigations on magnetically labeled hepatocyte transplantation or 3D cultures.

5. Conclusion

To the best of our knowledge, the present paper describes for the first time an *in vitro* evaluation of anionic iron oxide nanoparticle interaction with HepaRG cells. The magnetic

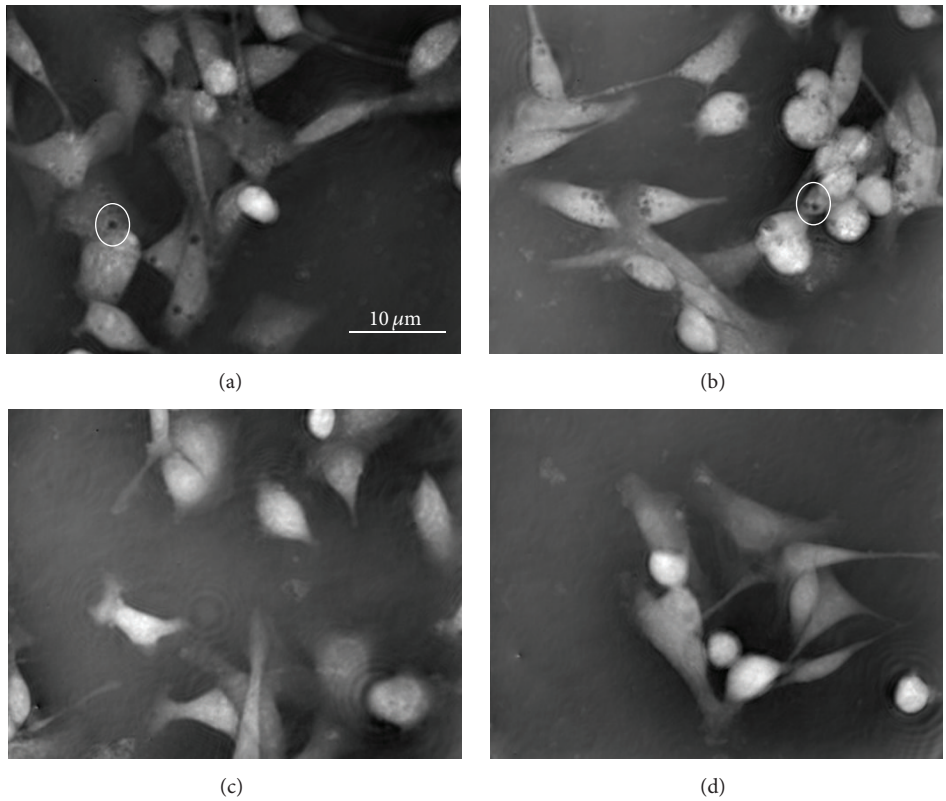

Figure 7: Holographic microscopy captures. (a) and (b) Visualization of internalized nanoparticles (circled dark points) into labeled HepaRG cells after an incubation time of 17 hours ([Fe] = 2 mM). (c) and (d) Control cells (no incubation with nanoparticles).

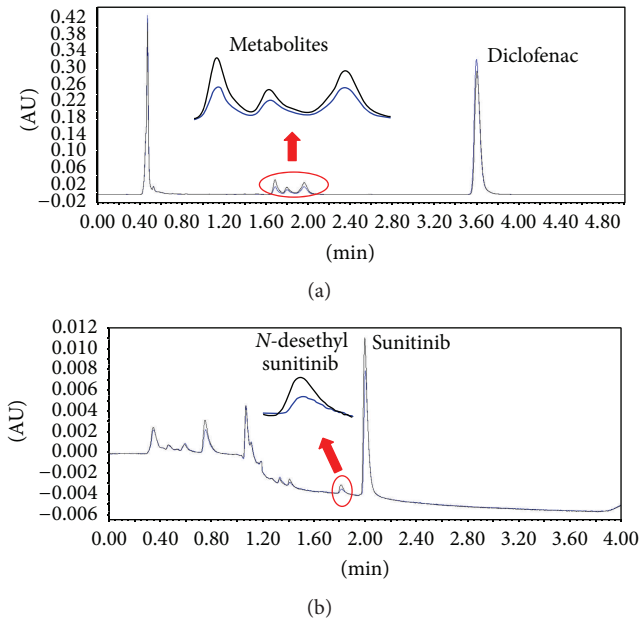

Figure 8: Typical chromatogram obtained with 250 μM diclofenac (a) and 20 μM sunitinib (b) metabolization tests during 5 hours or 6 hours, respectively. Unlabeled cells are represented in black color and labeled cells (17-hour incubation time with nanoparticles ([Fe] = 2 mM)) in blue color. Unlabeled cells gave higher metabolites areas than labeled cells.

labeling of this cell line was detected via microscopic observations (Prussian blue staining and holographic microscopy) and macroscopic (magnet influence) experiments.

Based on MTT assays (a good preliminary compound cytotoxicity indicator), the studied anionic iron oxide nanoparticles did not seem to exhibit cytotoxicity to the HepaRG cells for the investigated iron concentrations range (from 1 to 5 mM).

From the metabolization point of view, the HepaRG cells preserved their metabolic properties. As a slight decrease on drug metabolization activity of HepaRG cells was observed after their interaction with nanoparticles, further research works on tissue engineering have to take this point into account.

Conflict of Interests

The authors declare that there is no conflict of interests regarding the publication of this paper.

Acknowledgments

The authors are very grateful to the Department of General, Organic and Biomedical Chemistry, NMR, and Molecular Imaging Laboratory (Professor L. Vander Elst) for kindly providing them the nanoparticles used in this study. They

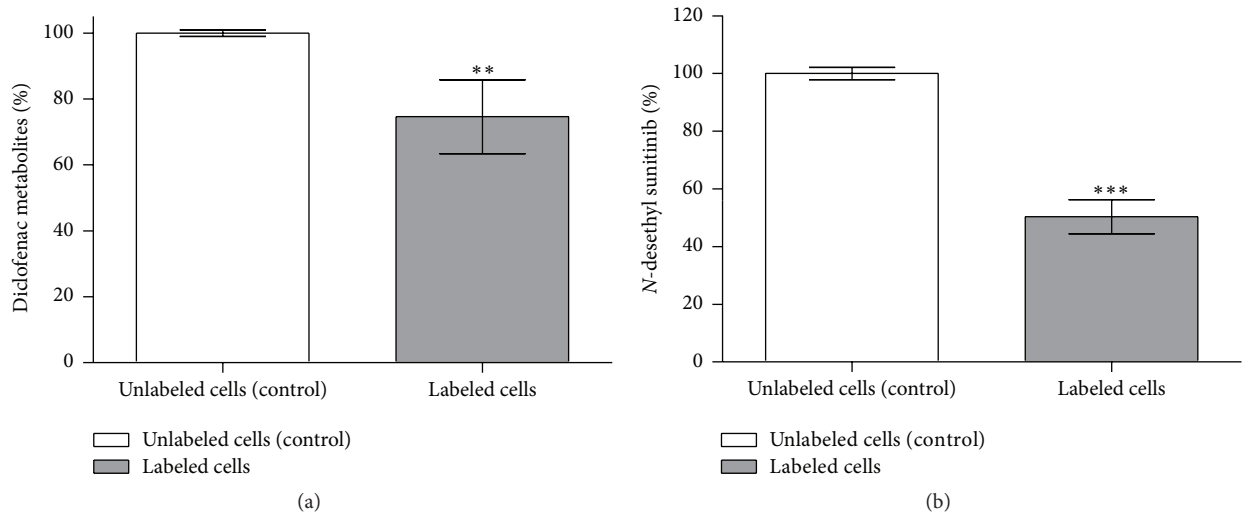

FIGURE 9: Histograms of diclofenac metabolites and *N*-desethyl sunitinib percentages after 5 hours and 6 hours of metabolization, respectively. Percentages were fixed at 100% for unlabeled cells. Statistically significant differences were observed with an unpaired *t*-test on metabolization activity by analysis of diclofenac metabolites ((a): $^{**}P < 0.01$) and *N*-desethyl sunitinib ((b): $^{***}P < 0.001$) peaks areas.

acknowledge FRMH (Fond pour la Recherche Médicale en Hainaut) and FNRS (Fond National de la Recherche Scientifique, FRSM Grant 3.4614.11) for their financial support. They also thank Ovizio Company for giving them the opportunity to have access to holographic microscopy. HepaRG cells (patented by Inserm Transfert) were supplied by Drs. Christiane Guguen-Guillouzo, Philippe Gripon, and Christian Trepo (INSERM's Laboratories U522 and U271) and used under a Material Transfer Agreement no. 10528B10 between INSERM U522 and U271 and the University of Mons, Belgium. They would like to acknowledge Biopredic International for their scientific help. The ARC (Research Contract AUWB-2010—10/15-UMONS-5), the FNRS, the Walloon Region, the COST TD1004 and TD1402, the UIAP VII program, and the Center for Microscopy and Molecular Imaging (CMMI, supported by the European Regional Development Fund and the Walloon Region) are thanked for their support.

References

[1] P. Gripon, S. Rumin, S. Urban et al., "Infection of a human hepatoma cell line by hepatitis B virus," *Proceedings of the National Academy of Sciences of the United States of America*, vol. 99, no. 24, pp. 15655–15660, 2002.

[2] V. Cerec, D. Glaise, P. Gripon, C. Guguen-Guillouzo, and A. Corlu, "C020—Capacité de transdifférenciation hépato-biliaire des cellules HepaRG issues d'un hépatocarcinome différencié et contrôles génétiques associés," *Gastroentérologie Clinique et Biologique*, vol. 29, no. 8-9, p. 893, 2005.

[3] V. Cerec, D. Glaise, D. Garnier et al., "Transdifferentiation of hepatocyte-like cells from the human hepatoma HepaRG cell line through bipotent progenitor," *Hepatology*, vol. 45, no. 4, pp. 957–967, 2007.

[4] A. Guillouzo, A. Corlu, C. Aninat, D. Glaise, F. Morel, and C. Guguen-Guillouzo, "The human hepatoma HepaRG cells: a highly differentiated model for studies of liver metabolism and toxicity of xenobiotics," *Chemico-Biological Interactions*, vol. 168, no. 1, pp. 66–73, 2007.

[5] K. P. Kanebratt and T. B. Andersson, "Evaluation of HepaRG cells as an in vitro model for human drug metabolism studies," *Drug Metabolism and Disposition*, vol. 36, no. 7, pp. 1444–1452, 2008.

[6] K. D. Hardy, M. D. Wahlin, I. Papageorgiou, J. D. Unadkat, A. E. Rettie, and S. D. Nelson, "Studies on the role of metabolic activation in tyrosine kinase inhibitor-dependent hepatotoxicity: induction of CYP3A4 enhances the cytotoxicity of lapatinib in HepaRG cells," *Drug Metabolism and Disposition*, vol. 42, no. 1, pp. 162–171, 2014.

[7] M. Turpeinen, A. Tolonen, C. Chesne, A. Guillouzo, J. Uusitalo, and O. Pelkonen, "Functional expression, inhibition and induction of CYP enzymes in HepaRG cells," *Toxicology in Vitro*, vol. 23, no. 4, pp. 748–753, 2009.

[8] S. Anthérieu, C. Chesné, R. Li et al., "Stable expression, activity, and inducibility of cytochromes P450 in differentiated HepaRG cells," *Drug Metabolism and Disposition*, vol. 38, no. 3, pp. 516–525, 2010.

[9] C. Aninat, A. Piton, D. Glaise et al., "CA50—expression d'enzymes de phase 1 et de phase 2 du métabolisme des xénobiotiques dans les cellules heparg dérivées d'un carcinome hépatocellulaire humain," *Gastroentérologie Clinique et Biologique*, vol. 29, no. 8-9, p. 924, 2005.

[10] M. Lübberstedt, U. Müller-Vieira, M. Mayer et al., "HepaRG human hepatic cell line utility as a surrogate for primary human hepatocytes in drug metabolism assessment in vitro," *Journal of Pharmacological and Toxicological Methods*, vol. 63, no. 1, pp. 59–68, 2011.

[11] J. Fraczek, J. Bolleyn, T. Vanhaecke, V. Rogiers, and M. Vinken, "Primary hepatocyte cultures for pharmaco-toxicological studies: at the busy crossroad of various anti-dedifferentiation strategies," *Archives of Toxicology*, vol. 87, no. 4, pp. 577–610, 2013.

[12] S. B. Leite, I. Wilk-Zasadna, J. M. Zaldivar et al., "Three-dimensional HepaRG model as an attractive tool for toxicity testing,"

Toxicological Sciences, vol. 130, no. 1, Article ID kfs232, pp. 106–116, 2012.

[13] D. Mueller, L. Krämer, E. Hoffmann, S. Klein, and F. Noor, "3D organotypic HepaRG cultures as in vitro model for acute and repeated dose toxicity studies," *Toxicology in Vitro*, vol. 28, no. 1, pp. 104–112, 2014.

[14] M. Darnell, T. Schreiter, K. Zeilinger et al., "Cytochrome P450-dependent metabolism in HepaRG cells cultured in a dynamic three-dimensional bioreactor," *Drug Metabolism and Disposition*, vol. 39, no. 7, pp. 1131–1138, 2011.

[15] G. A. A. Nibourg, R. Hoekstra, T. V. V. D. Hoeven et al., "Increased hepatic functionality of the human hepatoma cell line HepaRG cultured in the AMC bioreactor," *The International Journal of Biochemistry & Cell Biology*, vol. 45, no. 8, pp. 1860–1868, 2013.

[16] R. Hoekstra, G. A. A. Nibourg, T. V. Van Der Hoeven et al., "Phase 1 and phase 2 drug metabolism and bile acid production of HepaRG cells in a bioartificial liver in absence of dimethyl sulfoxide," *Drug Metabolism and Disposition*, vol. 41, no. 3, pp. 562–567, 2013.

[17] Q. A. Pankhurst, N. K. T. Thanh, S. K. Jones, and J. Dobson, "Progress in applications of magnetic nanoparticles in biomedicine," *Journal of Physics D: Applied Physics*, vol. 42, no. 22, Article ID 224001, 2009.

[18] C. Sun, J. S. H. Lee, and M. Zhang, "Magnetic nanoparticles in MR imaging and drug delivery," *Advanced Drug Delivery Reviews*, vol. 60, no. 11, pp. 1252–1265, 2008.

[19] G. R. Souza, J. R. Molina, R. M. Raphael et al., "Three-dimensional tissue culture based on magnetic cell levitation," *Nature Nanotechnology*, vol. 5, no. 4, pp. 291–296, 2010.

[20] K. Ino, A. Ito, and H. Honda, "Cell patterning using magnetite nanoparticles and magnetic force," *Biotechnology and Bioengineering*, vol. 97, no. 5, pp. 1309–1317, 2007.

[21] G. Frasca, F. Gazeau, and C. Wilhelm, "Formation of a three-dimensional multicellular assembly using magnetic patterning," *Langmuir*, vol. 25, no. 4, pp. 2348–2354, 2009.

[22] J. Dobson, "Remote control of cellular behaviour with magnetic nanoparticles," *Nature Nanotechnology*, vol. 3, no. 3, pp. 139–143, 2008.

[23] G. Frasca, F. Gazeau, and C. Wilhelm, "De la cellule au tissu: le magnétisme auxiliaire de la biomédecine," *Reflets de la Physique*, no. 23, pp. 6–10, 2011.

[24] L. Jong-Kook, I. Akira, and H. Hiroyuki, "Construction of functional cardiovascular tissues using magnetic nanoparticles," in *Cardiac Regeneration Using Stem Cells*, pp. 221–228, CRC Press, 2013.

[25] S. V. Pislaru, A. Harbuzariu, R. Gulati et al., "Magnetically targeted endothelial cell localization in stented vessels," *Journal of the American College of Cardiology*, vol. 48, no. 9, pp. 1839–1845, 2006.

[26] A. Ito, K. Ino, M. Hayashida et al., "Novel methodology for fabrication of tissue-engineered tubular constructs using magnetite nanoparticles and magnetic force," *Tissue Engineering*, vol. 11, no. 9-10, pp. 1553–1561, 2005.

[27] A. Ito, H. Jitsunobu, Y. Kawabe, and M. Kamihira, "Construction of heterotypic cell Sheets by magnetic force-based 3-D coculture of HepG2 and NIH3T3 cells," *Journal of Bioscience and Bioengineering*, vol. 104, no. 5, pp. 371–378, 2007.

[28] A. Luciani, A. Parouchev, P. Smirnov et al., "In vivo imaging of transplanted hepatocytes with a 1.5-T clinical MRI system—initial experience in mice," *European Radiology*, vol. 18, no. 1, pp. 59–69, 2008.

[29] A. Luciani, C. Wilhelm, P. Bruneval et al., "Magnetic targeting of iron-oxide-labeled fluorescent hepatoma cells to the liver," *European Radiology*, vol. 19, no. 5, pp. 1087–1096, 2009.

[30] C. Aninat, A. Piton, D. Glaise et al., "Expression of cytochromes P450, conjugating enzymes and nuclear receptors in human hepatoma HepaRG cells," *Drug Metabolism and Disposition*, vol. 34, no. 1, pp. 75–83, 2006.

[31] D. Stanicki, S. Boutry, S. Laurent et al., "Carboxy-silane coated iron oxide nanoparticles: a convenient platform for cellular and small animal imaging," *Journal of Materials Chemistry B*, vol. 2, no. 4, pp. 387–397, 2014.

[32] J.-L. Bridot, D. Stanicki, S. Laurent et al., "New carboxysilane-coated iron oxide nanoparticles for nonspecific cell labelling," *Contrast Media & Molecular Imaging*, vol. 8, no. 6, pp. 466–474, 2013.

[33] S. Boutry, D. Forge, C. Burtea et al., "How to quantify iron in an aqueous or biological matrix: a technical note," *Contrast Media & Molecular Imaging*, vol. 4, no. 6, pp. 299–304, 2009.

[34] M. Helvenstein, S. Hambÿe, and B. Blankert, "Determination of three tyrosine kinase inhibitors and one active metabolite by an identical and validated ultra-performance liquid chromatography-DAD method in human plasma," *Current Pharmaceutical Analysis*, vol. 10, no. 3, pp. 161–168, 2014.

[35] M. Rodamer, P. W. Elsinghorst, M. Kinzig, M. Gütschow, and F. Sörgel, "Development and validation of a liquid chromatography/tandem mass spectrometry procedure for the quantification of sunitinib (SU11248) and its active metabolite, *N*-desethyl sunitinib (SU12662), in human plasma: application to an explorative study," *Journal of Chromatography B*, vol. 879, no. 11-12, pp. 695–706, 2011.

[36] C. Wilhelm, F. Gazeau, J. Roger, J. N. Pons, and J.-C. Bacri, "Interaction of anionic superparamagnetic nanoparticles with cells: kinetic analyses of membrane adsorption and subsequent internalization," *Langmuir*, vol. 18, no. 21, pp. 8148–8155, 2002.

[37] C. Wilhelm, C. Billotey, J. Roger, J. N. Pons, J.-C. Bacri, and F. Gazeau, "Intracellular uptake of anionic superparamagnetic nanoparticles as a function of their surface coating," *Biomaterials*, vol. 24, no. 6, pp. 1001–1011, 2003.

[38] C. Wilhelm and F. Gazeau, "Universal cell labelling with anionic magnetic nanoparticles," *Biomaterials*, vol. 29, no. 22, pp. 3161–3174, 2008.

[39] P. P. Fu, Q. Xia, H.-M. Hwang, P. C. Ray, and H. Yu, "Mechanisms of nanotoxicity: generation of reactive oxygen species," *Journal of Food and Drug Analysis*, vol. 22, no. 1, pp. 64–75, 2014.

[40] M. C. Hohnholt and R. Dringen, "Iron-dependent formation of reactive oxygen species and glutathione depletion after accumulation of magnetic iron oxide nanoparticles by oligodendroglial cells," *Journal of Nanoparticle Research*, vol. 13, no. 12, pp. 6761–6774, 2011.